Scripta Materialia 140 (2017) 31–34

Contents lists available at ScienceDirect

Scripta Materialia

journal homepage: www.elsevier.com/locate/scriptamat

Regular article

Significant strengthening of nanocrystalline Ni sub-micron pillar by cyclic loading in elastic regime

Jung-A Lee [a], Dong-Hyun Lee [a], Moo-Young Seok [b], In-Chul Choi [c], Heung Nam Han [d], Ting Y. Tsui [e,*], Upadrasta Ramamurty [f], Jae-il Jang [a,*]

[a] Division of Materials Science and Engineering, Hanyang University, Seoul 04763, Republic of Korea
[b] Max-Planck-Institut für Eisenforschung GmbH, Max-Planck-Straße 1, Düsseldorf 40237, Germany
[c] Institute for Applied Materials, Karlsruhe Institute of Technology, Karlsruhe 76021, Germany
[d] Department of Materials Science and Engineering, Seoul National University, Seoul 08826, Republic of Korea
[e] Department of Mechanical Engineering, University of Waterloo, 200 University Avenue West, Waterloo, ON N21 3G1, Canada
[f] Department of Materials Engineering, Indian Institute of Science, Bangalore 560012, India

ARTICLE INFO

Article history:
Received 20 June 2017
Received in revised form 29 June 2017
Accepted 5 July 2017
Available online xxxx

Keywords:
Nanocrystalline metals
Micro-compression test
Cyclic loading

ABSTRACT

The influence of cyclic load, with the maximum stress well within the elastic regime, on the strength of nanocrystalline (nc) nickel was investigated through quasi-static compression experiments on cyclic-loaded sub-μm-sized pillars, fabricated through electron beam lithography and electroplating. Results show that prior-cycling enhances both yield and flow strengths of nc Ni without significant loss in plasticity. Changes in strain-rate sensitivity and activation volume for deformation upon cycling were measured and utilized to discuss possible mechanisms responsible for the observed strengthening.

The mechanical behavior of nanocrystalline (nc) metals with small volume such as nano-/micro-pillars is an active research topic, especially because there can be both extrinsic and intrinsic size effects (i.e., influences of pillar diameter, D and grain size, d) [1–8]. While extensive research, which was performed on these nc pillars hitherto, has uncovered plethora of interesting and exciting deformation behavior that arise as d is reduced to nm scale, most of it was performed under static or quasi-static loading conditions. However, the effect of cycling loading on the mechanical behavior (which is essential for ensuring reliability in structural applications where load fluctuations are common) of nc pillars remains unexplored although results of cyclic loading tests were reported for bulk samples of nc metals [9–12] or micro-pillars of single crystal and metallic glass [13–16].

Fatigue in crystalline metals is primarily a consequence of the kinematic irreversibility of slip [17]. Since nc metals offer more possibilities for such irreversibility to occur, by virtue of the large grain boundary (GB) area, their susceptibility for fatigue-induced property changes can be expected to be relatively more in comparison to their microcrystalline counterparts. Indeed, Moser et al. [9], who studied the cyclic plasticity of electrodeposited nc Ni (d = 40 nm), reported that cyclic loading leads to considerable hardening of the metal and attributed it to the dislocation source exhaustion at GBs. Molecular dynamics simulations by Rupert and Schuh [18] reported some evidence for strengthening in nc Ni (d = 3, 4, 5 and 10 nm). Only two cycles can cause grain rotation, which leads to enhanced boundary coherency, i.e., formation of GBs with low coincident site lattice values (Σ) such as Σ3 (twin boundary) that have lower energies and less stress concentration, which can lower the stress required for onset of plasticity otherwise.

Notably, Moser et al.'s experiments [9] were conducted wherein the maximum nominal stress of the tension-tension cyclic loading, S_{max}, exceeds the tensile yield strength, σ_y, of the nc Ni (see Fig. 1 of their paper). However, S_{max} does not need to necessarily exceed σ_y for kinematic irreversibility to set in; the fact that the endurance limit of most metals can be as low as 0.35 to 0.5 times σ_y is a testament for this. Further, and already mentioned, nc metals can offer more avenues for fatigue induced irreversible microstructural changes. Therefore, it is reasonable to anticipate that cyclic loading, even when S_{max} is well below σ_y, i.e., the deformation during cycling being nominally elastic, can significantly alter the mechanical behavior of the metals.

We critically examine this possibility by conducting experiments on sub-μm-sized pillars of nc Ni that were prepared through high-throughput electron beam lithography and electroplating process [19]. A series of cyclic and subsequent monotonic micro-compression tests reveal that both yield strength and flow stress significantly increase because of prior-cyclic loading. Mechanistic origins for the observed hardening are discussed in terms of strain-rate sensitivity, and activation volume for deformation, etc.

* Corresponding authors.
E-mail addresses: tttsui@uwaterloo.ca (T.Y. Tsui), jijang@hanyang.ac.kr (J. Jang).

http://dx.doi.org/10.1016/j.scriptamat.2017.07.001
1359-6462/

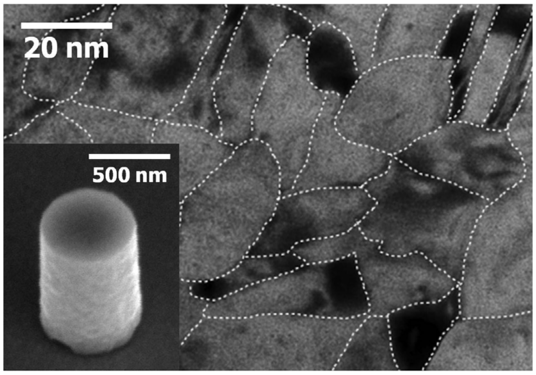

Fig. 1. Representative TEM image showing the grain structure of as-fabricated nc Ni pillars (with inset of SEM image for pillar morphology).

The sub-μm-sized nc Ni pillars examined in this study were prepared through electron beam lithography and electroplating techniques [19]. Thin ~20 nm Ti (adhesion layer) and ~40 nm Au (conductive seed layer) were sequentially deposited on silicon substrates, that were subsequently spin coated by polymethylmethacrylate (PMMA) resist. Arrays of ~580 nm diameter via-holes were patterned on the resist using electron beam lithography and then filled nc Ni by electroplating (with the exposed Au layer acting as the cathode and a commercial grade pure Ni as the anode). The Ni plating solution was made of Ni (II) sulfate hexahydrate (99%, Sigma Aldrich, St. Louis, MO), Ni (II) chloride (98%, Sigma Aldrich), boric acid (BX0865, EMD Millipore), and organic additive saccharin (98%, Sigma Aldrich). After plating, the PMMA resist was dissolved in a bath of acetone, to obtain nc Ni pillars. This fabrication technique has many advantages over that which used focused ion beam (FIB) milling. For example, hundreds of highly uniform pillars can be produced at the same time (which saves time and cost, and allows for statistically significant amount of experimentation and data analysis [8,20]). Importantly, one does not need to worry at all about the usual concern of surface damage that arises when FIB milled micropillars are used. The morphologies and microstructures of pillars were observed using scanning and transmission electron microscopies (SEM: JSM-6330F, and TEM: JEM-2010F, both equipment from JEOL Ltd., Tokyo, Japan), respectively.

Cyclic and subsequent quasi-static compression tests of the pillars were conducted using Nanoindenter XP (formerly MTS; now Keysight, Santa Rosa, CA) equipped with a FIB-milled cylindrical diamond punch. Compression-compression cyclic loading was performed up to a predetermined number of cycles, N (=10, 20, 100 and 200), with S_{max} of 1000 MPa (that is below σ_y ~ 1.6–1.8 GPa) with a stress ratio R (=S_{min} / S_{max} where S_{min} is the minimum stress) of 0.1 at a frequency λ of 0.5 Hz. In order to directly observe the possible change in pillar morphology during cyclic loading, in-situ compression tests were conducted by using a PI 85 picoindenter (Hysitron Inc., Mineapolis, MN) set inside a Quanta 250 FEG scanning electron microscope (FEI Inc., Hillsboro, OR). Quasi-static compression tests of both as-fabricated and cyclic-loaded pillars were performed under different nominal strain rates, $\dot{\varepsilon}$, of 0.0005, 0.002, and 0.005 s^{-1}. More than 10 measurements were conducted for each condition so as to obtain data with fidelity. Thermal drift was maintained below 0.03 nm/s in all the experiments.

A representative micrograph of the pillar was displayed in the inset of Fig. 1. The top surfaces of the pillars are flat while the side-surfaces are almost taper-free. The nominal outer diameter, D, of the pillars is ~580 nm and the height-to-diameter aspect ratio is ~1.5. A TEM image of the representative microstructure of as-fabricated pillars is displayed in Fig. 1. The average grain size, d, was determined as ~12 ± 3 nm, which was measured using multiple TEM micrographs taken at various locations of each pillar.

The pillars were subjected to compression-compression cyclic loading with sawtooth shape waveform (Fig. 2a). From the applied load, P,

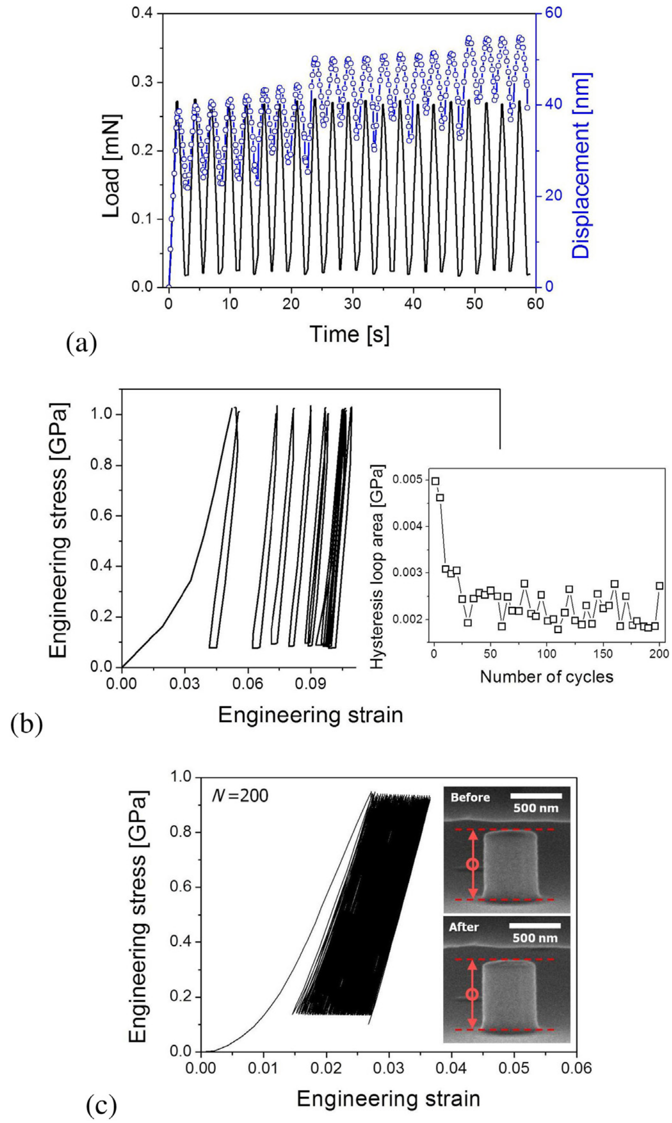

Fig. 2. Results of cyclic tests: (a) load vs. time and displacement vs. time obtained during cyclic loading; (b) converted engineering stress-strain responses with inset of hysteresis loop area as a function of N; (c) the curve from in-situ SEM experiments and the SEM images taken before and after cyclic loading.

and displacement, h, responses recorded, engineering stress, S (=P / A_0, where A_0 is the initial cross-sectional area of pillar) vs. engineering strain, e (=h / L_0 where L_0 is the initial pillar height) were obtained. An example of S–e response is shown in Fig. 2b (for N = 200, which is the maximum N applied in this study). Note that $S_{max} \ll \sigma_y$ (~1.6–1.8 GPa), i.e., deformation during the entire cycling is well within the elastic limit. For clarity, only the data for every 20 cycles are shown in Fig. 2b. Hysteresis was observed during early cycles. The width of the loops reaches a steady state at N of ~30. The area of the hysteresis loop, $\Delta\Gamma$, a measure of the strain energy dissipated during that cycle, is evaluated and plotted as a function of N in the inset of Fig. 2b. It shows that $\Delta\Gamma$ decreases markedly within the first 20 cycles or so, before becoming negligible. To directly visualize cyclic deformation (if any), in-situ cyclic tests were performed under identical experimental conditions (S_{max} = 1 GPa, R = 0.1, λ = 0.5 Hz, and N = 200) while the pillars were imaged (see the corresponding movie in Supplementary material). In Fig. 2c, the obtained S–e curve and representative SEM images of a pillar before and after in-situ cyclic tests are displayed. The geometry of the pillar remains apparently unchanged, indicating the absence of noticeable plastic deformation or localized failure until N = 200.